

International Journal of Modern Physics D  
© World Scientific Publishing Company

## Correlation of structure growth index with current cosmic acceleration, and Padé dark energy parameterizations

G. Panotopoulos

*Centro de Astrofísica e Gravitação-CENTRA, Instituto Superior Técnico-IST, Universidade de Lisboa-UL, Av. Rovisco Pais, 1049-001 Lisboa, Portugal.*

*Departamento de Ciencias Físicas, Universidad de la Frontera, Casilla 54-D, 4811186 Temuco, Chile.*

*grigorios.panotopoulos@ufrontera.cl*

G. Barnert

*Departamento de Astronomía, FCFM, Universidad de Chile, Camino El Observatorio 1515, Las Condes, Santiago, Chile.*

*gerald\_barnert@hotmail.com*

L. E. Campusano

*Departamento de Astronomía, FCFM, Universidad de Chile, Camino El Observatorio 1515, Las Condes, Santiago, Chile.*

*luis@das.uchile.cl*

Received Day Month Year

Revised Day Month Year

We study dynamical dark energy models within Einstein's theory by means of matter perturbations and the growth index  $\gamma$ . Contrary to the common approach, here we start assuming a linear ansatz for the growth index, and we investigate its impact on the deceleration parameter,  $q$ , as well as on the dark energy equation-of-state parameter,  $w$ . Following this approach we find a relationship between today's value  $q_0$  and  $\gamma$ , which to the best of our knowledge had not been obtained before. We find that in most of the cases,  $w(z)$  crosses the -1 line (quintom) ending at a present day value  $w_0 > -1$ . Furthermore, we show that an analytic expression for the dark energy equation-of-state parameter may be obtained in the form of order (4,4) (or higher) Padé parameterizations.

*Keywords:* Dark energy; General Relativity; Evolution of perturbations; Growth index.

### 1. Introduction

The origin and nature of dark energy (DE), the fluid component that currently accelerates the Universe,<sup>1-3</sup> is one of the biggest mysteries and challenges in modern theoretical Cosmology. It is well-known that according to the cosmological equations within Einstein's General Relativity,<sup>4</sup> a Universe consisting of radiation and non-relativistic matter only cannot expand at an accelerating rate. On the contrary, a non-vanishing (and positive) cosmological constant<sup>5,6</sup> has been proven to be the

most economical model in an overall excellent agreement with a wealth of available observational data.

The  $\Lambda$ CDM model, based on collisionless dark matter and a positive cosmological constant, despite its successes, does not come without problems. In modern times the community is facing two puzzles, one related to the cosmological constant problem<sup>7,8</sup> and the other to the Hubble tension. To be more precise, regarding the value of the Hubble constant  $H_0$ , there is nowadays a disagreement between determinations based on the high red-shift CMB data and on measurements at low red-shift respectively, see e.g.<sup>9–12</sup> The value of the Hubble constant determined by the PLANCK Collaboration,<sup>13,14</sup>  $H_0 = (67 - 68)$  km/(Mpc sec), is found to be significantly lower than the value obtained by local measurements,  $H_0 = (73 - 74)$  km/(Mpc sec).<sup>15,16</sup> This disagreement might call for new physics.<sup>17–19</sup> For an excellent recent review on challenges for the  $\Lambda$ CDM model see.<sup>20</sup>

As originally discussed by Schutz,<sup>21</sup> inspiraling compact neutron star or black hole binaries are excellent standard sirens, in that their gravitational wave measurements could determine the sources absolute distances. Moreover, recent observations have accumulated compelling evidence that some short gamma-ray bursts are associated with the mergers of neutron star binaries.<sup>22</sup> Hence, simultaneous observations of the inspiraling gravitational waves and of signatures in the electromagnetic band may allow a direct and independent determination of both the luminosity distance and the red-shift to a binary.<sup>22</sup> Furthermore, the latter through the expression of a second order Taylor expansion for the luminosity distance as a function of red-shift,  $d_L(z)$ <sup>15,23</sup>

$$d_L(z) \approx \frac{z}{H_0} \left[ 1 + \frac{z}{2}(1 - q_0) \right], \quad (1)$$

would allow for an independent determination of the Hubble constant  $H_0$ ,<sup>24</sup> and at the same time an allowed range on  $q_0$ ,<sup>23</sup> which stems from a  $(q_0 - j)$  parameterization, with  $j$  being the jerk parameter.

Due to the problems related to the cosmological constant, as was to be expected, a plethora of several different dark energy models have been proposed and studied over the years as possible alternatives to the  $\Lambda$ CDM model. Quite generically, all dark energy models are classified into two broad classes. On the one hand, there is a family of models related to alternative/modified theories of gravity, where new correction terms appear to GR at cosmological scales. And on the other hand, in another family of models, a new dynamical field with an equation-of-state (EoS) parameter  $w < -1/3$  is introduced. In the first class of models, called geometrical DE, one finds for instance  $f(R)$  theories of gravity,<sup>25–28</sup> brane-world models<sup>29–31</sup> and Scalar-Tensor theories of gravity,<sup>32–35</sup> while in the second class, called dynamical DE, one finds models such as quintessence,<sup>36</sup> phantom,<sup>37,38</sup> quintom,<sup>39,40</sup> tachyonic<sup>41</sup> or k-essence.<sup>42</sup> For an excellent review on the dynamics of dark energy see e.g.<sup>43</sup>

Depending on the details of the underlying theory of gravity and/or the properties of the assumed DE model, the evolution of linear matter perturbations may be affected in several ways. Even if two DE models give the same late-time accelerating expansion, they still may differ in the matter perturbations they produce.<sup>44,45</sup> This fact could provide an additional important way to discriminate at low red-shift between various DE models (see e.g.<sup>46–49</sup>). It is therefore important to characterize as accurately as possible the growth of matter perturbations. A quantity that has been studied considerably over the years is the so called growth index,  $\gamma$ , introduced in.<sup>50</sup> In fact, the growth rate of matter perturbations could be probed by means of three dimensional weak lensing surveys.<sup>51</sup>

In the present work we study in detail the growth of matter perturbations, and give a thorough discussion on the correlation between a linear ansatz for the growth index with both the deceleration parameter and the DE equation-of-state parameter. Contrary to the common approach in which one first assumes a concrete DE model and then solves the equation for the matter density contrast to compute the growth index, here we follow the inverse approach, namely first we assume a linear ansatz for the growth index, and then investigate its impact on properties of dark energy, integrating numerically the equation for matter perturbations assuming a homogeneous (i.e. it does not cluster) dark energy. What is more, to the best of our knowledge, we use here a relatively new constraint on the deceleration parameter coming from standard sirens to put bounds on the growth index.

Our plan in the present article is the following: In the next section we briefly review the standard Friedmann-Robertson-Walker Universe at background level as well as the linear cosmological perturbations. In section 3 we show and discuss our main numerical results. Finally, in section 4 we close with some concluding remarks. We adopt the mostly positive metric signature,  $(-, +, +, +)$ , and work in units where the speed of light in vacuum is set to unity,  $c = 1$ .

## 2. Theoretical framework

The starting point is Einstein's GR<sup>4</sup> based on the Einstein-Hilbert term coupled to the matter content

$$S = \int d^4x \sqrt{-g} \left[ \frac{R}{16\pi G} + \mathcal{L}_M \right] \quad (2)$$

where  $g_{\mu\nu}$  is the metric tensor,  $g$  is its determinant,  $R$  is the corresponding Ricci scalar,  $G$  is Newton's constant and  $\mathcal{L}_M$  is the Lagrangian of the matter content. Varying the action with respect to the metric tensor one obtains the well-known Einstein's field equations, which read

$$G_{\mu\nu} \equiv R_{\mu\nu} - \frac{1}{2} R g_{\mu\nu} = 8\pi G T_{\mu\nu} \quad (3)$$

where  $R_{\mu\nu}$  is the Ricci tensor, while  $T_{\mu\nu}$  is the matter energy-momentum tensor.

### 2.1. Background evolution

The basic cosmological equations governing the expansion of a homogeneous and isotropic Universe may be found e.g. in.<sup>52</sup> Although they are standard textbook expressions, to set the notation and for self-completeness, we collect here the equations we use in the numerical analysis to be presented in section III.

If matter consists of a perfect fluid with **total** pressure  $p$  and **total** energy density  $\rho$ , the energy momentum tensor is given by

$$T_{\mu\nu} = p g_{\mu\nu} + (p + \rho) u_\mu u_\nu \quad (4)$$

where  $u_\mu$  is the four-velocity of the fluid satisfying the condition  $u_\mu u^\mu = -1$ . The mixed component stress-energy tensor takes the form<sup>52</sup>

$$T^\mu_\nu = \text{diag}(-\rho, p, p, p) \quad (5)$$

A spatially flat, isotropic and homogeneous Universe is described by a Robertson-Walker metric<sup>52</sup>

$$ds^2 = -dt^2 + a(t)^2 \delta_{ij} dx^i dx^j \quad (6)$$

where the scale factor,  $a(t)$ , is the only unknown function, and all quantities of interest, such as  $p, \rho$ , depend on the cosmic time  $t$  only.

The cosmological equations are found to be the continuity equation as well as the two Friedmann equations<sup>52</sup>

$$H^2 = \frac{8\pi G}{3} \rho \quad (7)$$

$$\frac{\ddot{a}}{a} = -\frac{4\pi G}{3} (\rho + 3p) \quad (8)$$

or equivalently

$$\dot{H} = -4\pi G(\rho + p) \quad (9)$$

$$0 = \dot{\rho} + 3H(\rho + p) \quad (10)$$

where an over dot denotes differentiation with respect to cosmic time, and  $H = \dot{a}/a$  is the Hubble parameter.

It is more convenient to introduce for each fluid component  $X$  the normalized (dimensionless) density,  $\Omega_X$ , which is defined to be

$$\Omega_X \equiv \frac{\rho_X}{\rho_c}, \quad \rho_c = \frac{3H^2}{8\pi G}, \quad (11)$$

and therefore the first Friedmann equation may be written down equivalently as a constraint of the following form

$$\sum_X \Omega_X = 1 \quad (12)$$

i.e. the normalized densities of all fluid components sum up to unity.

In particular, the matter normalized density as a function of the scale factor takes the form

$$\Omega_m(a) = \frac{\Omega_{m,0}}{a^3 E(a)^2} \quad (13)$$

where  $\Omega_{m,0}$  is the matter normalized density evaluated at today, while the dimensionless Hubble parameter,  $E(a)$ , is given by

$$E(a)^2 \equiv \left( \frac{H(a)}{H_0} \right)^2 = \Omega_{m,0} a^{-3} + (1 - \Omega_{m,0}) F(a) \quad (14)$$

neglecting radiation at late times, where  $H_0$  is the Hubble parameter evaluated at today, and  $F(a)$  is determined by the DE equation-of-state parameter as follows

$$w(z) = -1 + (1+z) \frac{F'(z)}{3F(z)}. \quad (15)$$

Clearly, the present value of both  $E(a)$  and  $F(a)$  equals to unity

$$E(a=1) = 1, \quad F(a=1) = 1. \quad (16)$$

Finally, the deceleration parameter,  $q$ , is defined by

$$q \equiv -\frac{\ddot{a}}{aH^2} \quad (17)$$

while as a function of red-shift,  $z = -1 + a_0/a$ , with  $a_0$  being the present value of the scale factor, it is computed to be

$$q(z) = -1 + (1+z) \frac{H'(z)}{H(z)}. \quad (18)$$

In the following, instead of the cosmic time we shall be using either the scale factor,  $a$ , or the red-shift,  $z$ , as the independent variable.

## 2.2. Linear cosmological perturbations

Let us briefly review linear cosmological perturbation theory within GR, see e.g.<sup>53,54</sup>

The goal is to solve the perturbed Einstein's field equations

$$\delta G^\mu_\nu = 8\pi G \delta T^\mu_\nu \quad (19)$$

On the one hand, for scalar perturbations relevant in growth of structures, the metric tensor has the form

$$ds^2 = -(1 + 2\Psi)dt^2 + (1 - 2\Psi)\delta_{ij}dx^i dx^j \quad (20)$$

where  $\Psi$  is the metric perturbation, while for the cosmological fluid the perturbed stress-energy tensor has the form

$$\delta T^0_0 = \delta\rho, \quad \delta T^i_j = -\delta p \delta^i_j \quad (21)$$

The full set of coupled equations for matter and metric perturbations may be found e.g. in.<sup>55-57</sup>

The Fourier transform of the density contrast,  $\delta_k = \delta\rho_m/\rho_m$ , with  $k$  being the wave number, for pressure-less matter satisfies the following linear differential equation<sup>58–60</sup>

$$\ddot{\delta}_k + 2H\dot{\delta}_k - 4\pi G\rho_m\delta_k = 0 \quad (22)$$

at linear level assuming that DE does not cluster (homogeneous DE),  $\delta_k \ll 1$ , and for sub-horizon scales,  $k/(2\pi a) \gg aH$ , when only non-relativistic matter clusters. During matter domination

$$a(t) \sim t^{2/3}, \quad H(t) = \frac{2}{3t} \quad (23)$$

the matter density contrast grows linearly with the scale factor,  $\delta_k(a) \sim a$ .

The equation for  $\delta$  may be take equivalently the following form

$$\delta''(a) + \left(\frac{3}{a} + \frac{E'(a)}{E(a)}\right)\delta'(a) - \frac{3}{2} \frac{\Omega_m}{a^5 E(a)^2} \delta(a) = 0 \quad (24)$$

where for simplicity we drop the sub-index  $k$ , a prime denotes differentiation with respect to the scale factor.

The growth index,  $\gamma$ , is defined to be

$$f \equiv \frac{d \ln \delta}{d \ln a} = \frac{a}{\delta} \frac{d\delta}{da} \quad (25)$$

$$f = \Omega_m^\gamma \quad (26)$$

or equivalently

$$\gamma(a) = \frac{\ln(f(a))}{\ln(\Omega_m(a))} \quad (27)$$

For a constant DE equation-of-state,  $w(z) = w$ , there is an impressive agreement between the numerical result and an analytic approximation, and at lowest order it is computed to be<sup>59</sup>

$$\gamma = \frac{3(w-1)}{6w-5} \quad (28)$$

around  $z \sim 1$ . This reduces to  $\gamma = 6/11$  for  $\Lambda$ CDM ( $w = -1$ ). In full generality, however, the growth index is a function of red-shift, with a non-vanishing derivative  $\gamma'(z) \equiv d\gamma(z)/dz$ . In an attempt to further improve on the analytic approximation, in<sup>45, 59</sup> those authors considered an expansion to first order in  $z$  of the form

$$\gamma(z) = \gamma_0 + \gamma_1 z \quad (29)$$

which could have interesting observational consequences, and which is characterized by two parameters that may be identified with today's values of the functions  $\gamma(z), \gamma'(z)$

$$\gamma_0 = \gamma(z=0), \quad \gamma_1 = \gamma'(z=0) \quad (30)$$

During matter domination, since  $\delta \propto a$ , by definition  $f$  is found to be  $f(a) = 1$ . Furthermore, the second order differential equation for  $\delta$  may be written down equivalently as a first order differential equation for  $f(a)$  as follows

$$af'(a) + f(a)^2 + f(a) \left( 2 + a \frac{E'(a)}{E(a)} \right) = \frac{3\Omega_m(a)}{2}. \quad (31)$$

### 3. Numerical results

As already mentioned, in the present work instead of adopting a specific DE model, i.e. a given parameterization  $w(a)$  or  $w(z)$ , we assume, following<sup>45,59</sup> that the evolution of matter perturbations implies a linear growth index on the red-shift space of the form eq. (29) of the previous section, valid at low red-shift in the range  $0 \leq z \leq 1$ . The parameters  $\gamma_0, \gamma_1$  typically vary in the range<sup>45</sup>

$$0.5 < \gamma_0 < 0.6, \quad -0.05 < \gamma_1 < 0.05, \quad (32)$$

and we investigate what the impact of those two free parameters is on properties of DE, such as the equation-of-state parameter,  $w(z)$ , and on the deceleration parameter evaluated at present,  $q_0$ . In contrast to,<sup>45</sup> where only an algebraic equation relating  $w_0, \gamma_0, \gamma_1$  was considered, we integrate numerically the equation for matter perturbations, and determine how both  $q$  and  $w$  evolve with red-shift. Moreover, we put bounds on  $\gamma$  using an allowed range on  $q_0$  that stems from a  $(q_0 - j)$  parameterization,<sup>23</sup> with  $j$  being the jerk parameter.

Let us briefly describe the approach followed here. Since the DE model is a priori unknown, all quantities of interest may be expressed in terms of the unknown function  $F(a)$ , which is directly related to the DE equation-of-state  $w(a)$ . The differential equation for  $f(a)$  may be viewed as a differential equation for  $F(a)$  instead, subjected to the initial condition  $F(a = 1) = 1$ . Once the numerical values of  $\Omega_{m,0}, \gamma_0, \gamma_1$  are specified, the differential equation may be integrated numerically, and after that  $q(z)$  and  $w(z)$  may be computed in a straightforward manner.

Our main numerical results are displayed in the figures below. Throughout the numerical analysis we set  $\Omega_{m,0} = 0.3$ , and we vary both  $\gamma_0$  and  $\gamma_1$ . In the left panel of Fig. 1 we show  $q_0$  versus  $\gamma_1$  for a given  $\gamma_0$ . The three different curves correspond to distinct numerical values of  $\gamma_0 = 0.52, 0.55, 0.59$  from bottom to top. For a given  $\gamma_0$ ,  $q_0$  decreases almost linearly with  $\gamma_1$ , while as  $\gamma_0$  increases the curves are displaced upwards, and they are less rapidly varying functions of  $\gamma_1$ . It is worth mentioning that the curve for  $\gamma_0 = 0.52$  is considerably displaced downwards with respect to the other two.

Similarly, in the right panel of Fig. 1 we show  $q_0$  versus  $\gamma_1$  for a fixed  $\gamma_0 = 0.55$ , and include a horizontal strip corresponding to the allowed range  $q_0 = -0.50 \pm 0.08$ . Thus, we obtain for  $\gamma_1$  the constraint  $-0.042 \leq \gamma_1 \leq -0.029$ . For the two extreme values corresponding to the lower and upper bound of  $\gamma_1$ , we show in the bottom panel of Fig. 1 the equation-of-state parameter  $w(z)$ . In the case represented

by the cyan curve,  $w(z)$  remains always below the  $-1$  line, and therefore DE is phantom.<sup>37,38</sup> At a more fundamental level based on a Lagrangian description, this class of dynamical DE model may be analyzed introducing a real scalar field with the "wrong" sign in front of its kinetic term. On the other hand, the case represented by the orange curve crosses the  $-1$  line, and therefore DE is quintom.<sup>39,40</sup> This time again at a more fundamental level based on a Lagrangian description, this class of dynamical DE model may be analyzed introducing two real scalar fields, one minimally coupled and another with the "wrong" sign in front of its kinetic term.<sup>61,62</sup>

Next, the impact of the  $\gamma_1$  variation on  $q(z)$  (left panel) and  $w(z)$  (right panel) is shown in Fig. 2 setting  $\gamma_0 = 0.55$  and  $\Omega_{m,0} = 0.3$ . We have considered four different values of  $\gamma_1 = -0.04, -0.02, 0.02, 0.04$ . The equation-of-state parameter crosses the  $-1$  line (quintom) either from lower to higher values when  $\gamma_1$  is negative or from higher to lower values when  $\gamma_1$  is positive. Moreover, both  $q_0$  and the transition red-shift,  $z_*$ , between deceleration and acceleration decrease with  $\gamma_1$ . It is worth noticing that in both panels of Fig. 2, all four curves meet (approximately) at the same point. We have checked that this point corresponds to the point at which  $\Omega_m = \Omega_{DE}$  (see Fig. 3), which is not sensitive to  $\gamma_1$ , although at the moment we do not have an explanation to offer as to why this happens. If it is not a coincidence, it certainly deserves further and careful examination.

Finally, a comment is in order at this stage. Within our approach the DE equation-of-state may be obtained numerically. However, it would be both desirable and advantageous to have an analytic expression for  $w(z)$ . One way to do that is to fit the function  $F(z)$  with a polynomial of degree  $n$ ,  $F(z) \approx P_n(z)$ . Recall that  $F(z)$  is directly related to  $w(z)$ . Then it is easy to verify that the DE equation-of-state parameter takes the form of a  $(m, n)$  Padé parameterization,<sup>63</sup> which only recently is discussed in the literature concerning cosmology and DE (see e.g.<sup>64,65</sup>), and which quite generically for any function  $h(z)$  is given by<sup>66,67</sup>

$$h(z) = \frac{R_n(z)}{Q_m(z)} = \frac{c_0 + c_1 z + \dots + c_n z^n}{d_0 + d_1 z + \dots + d_m z^m}, \quad (33)$$

namely a rational function where both the numerator and the denominator are polynomials of degree  $n$  and  $m$ , respectively.

To evaluate the goodness of the polynomial fits, namely to check if the fit to a polynomial is a good one, we compute the relative errors with respect to the numerical solution, and we require that it does not exceed 5% in order for the fit to be a satisfactory one. Although this choice is arbitrary, we consider it to be informative, while at the same time it is not too restrictive.

We have carefully checked that low degree polynomials are not acceptable according to such a criterion, and show that the Padé approximation for the DE EoS parameter must be at least (4,4), in contrast to the analysis performed in a previous related work,<sup>64</sup> where a (1,1) Padé parameterization was considered. The main differences between that work and ours are the following. First, the ansatz for  $\gamma(z)$



in<sup>64</sup> was not a linear one. Moreover, here we integrate the equation for matter perturbations numerically, whereas in<sup>64</sup> an analytical approach, developed in,<sup>68</sup> was followed.

For instance, in the case where  $\Omega_{m,0} = 0.3$ ,  $\gamma_0 = 0.55$  and  $\gamma_1 = -0.029$ , we find the following analytic expression for  $w(z)$

$$w(z) = \frac{R_4(z)}{Q_4(z)}, \quad (34)$$

$$R_4(z) = 0.33z^4 + 1.33z^3 - 1.98z^2 - 0.03z - 3.25, \quad (35)$$

$$Q_4(z) = z^4 - 2.08z^3 - 0.29z^2 - 0.25z + 3.17, \quad (36)$$

while in the case where  $\Omega_{m,0} = 0.3$ ,  $\gamma_0 = 0.55$  and  $\gamma_1 = -0.042$ , we find the following analytic expression for  $w(z)$

$$w(z) = \frac{R_5(z)}{Q_5(z)}, \quad (37)$$

$$R_5(z) = 0.65z^5 + 1.34z^4 - 1.29z^3 + 0.09z^2 - 1.37z - 1.32, \quad (38)$$

$$Q_5(z) = z^5 - 0.97z^4 - 0.4z^3 - 1.46z^2 + 0.59z + 1.52. \quad (39)$$

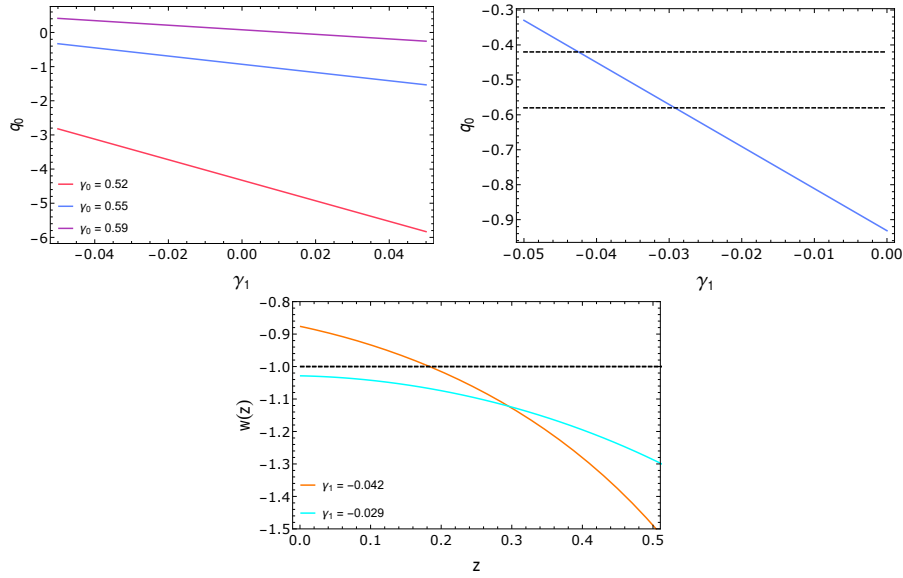


Fig. 1. **Top left:** Deceleration parameter evaluated at today,  $q_0$ , versus  $\gamma_1$  for  $\Omega_{m,0} = 0.3$  and  $\gamma_0 = 0.52, 0.55, 0.59$ . **Top right:**  $q_0$  versus  $\gamma_1$  for  $\Omega_{m,0} = 0.3$  and  $\gamma_0 = 0.55$ . The limits  $q_0 = -0.5 \pm 0.08$  are shown as well. **Bottom:** Equation-of-state parameter,  $w$ , versus red-shift,  $z$ , for  $\Omega_{m,0} = 0.3$ ,  $\gamma_0 = 0.55$  and  $\gamma_1 = -0.042$  (orange color) and  $\gamma_1 = -0.029$  (cyan color).

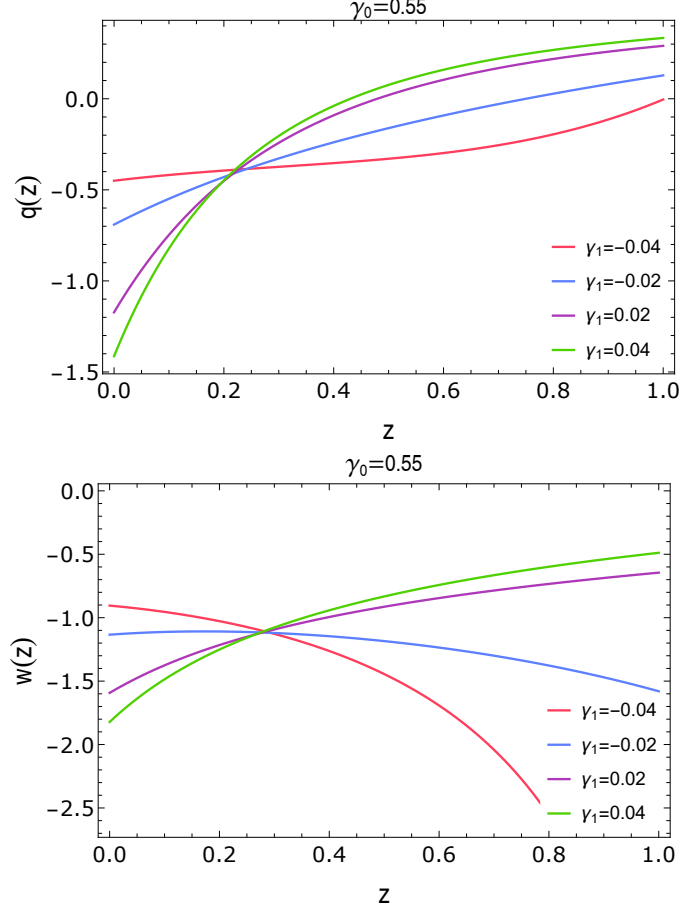


Fig. 2. **TOP:** Deceleration parameter,  $q$ , versus red-shift,  $z$ , for  $\Omega_{m,0} = 0.3, \gamma_0 = 0.55$  and  $\gamma_1 = -0.04, -0.02, 0.02, 0.04$ . **BOTTOM:** Equation-of-state parameter,  $w$ , versus red-shift,  $z$ , for  $\Omega_{m,0} = 0.3, \gamma_0 = 0.55$  and  $\gamma_1 = -0.04, -0.02, 0.02, 0.04$ .

#### 4. Conclusions

In summary, the present work has been devoted to the study of dynamical DE models within four-dimensional GR. Assuming that DE does not cluster (homogeneous DE), the starting point was the differential equation for the density contrast of non-relativistic matter. Instead of the usual treatment, where one assumes a concrete DE model to compute the growth index, here we followed the inverse approach. Specifically, we first assumed for  $\gamma(z)$  a linear ansatz  $\gamma(z) = \gamma_0 + \gamma_1 z$  valid at low red-shift,  $0 < z < 1$ , and then investigated its impact on the properties of DE. Within this approach we have found a relationship between  $q_0$  and  $\gamma$ , which to the best of our knowledge had not been obtained before. Our main numerical results reveal that for  $\Omega_{m,0}, \gamma_0$  fixed,  $q_0$  is a decreasing function of  $\gamma_1$ , whereas for a given  $\gamma_1$ ,

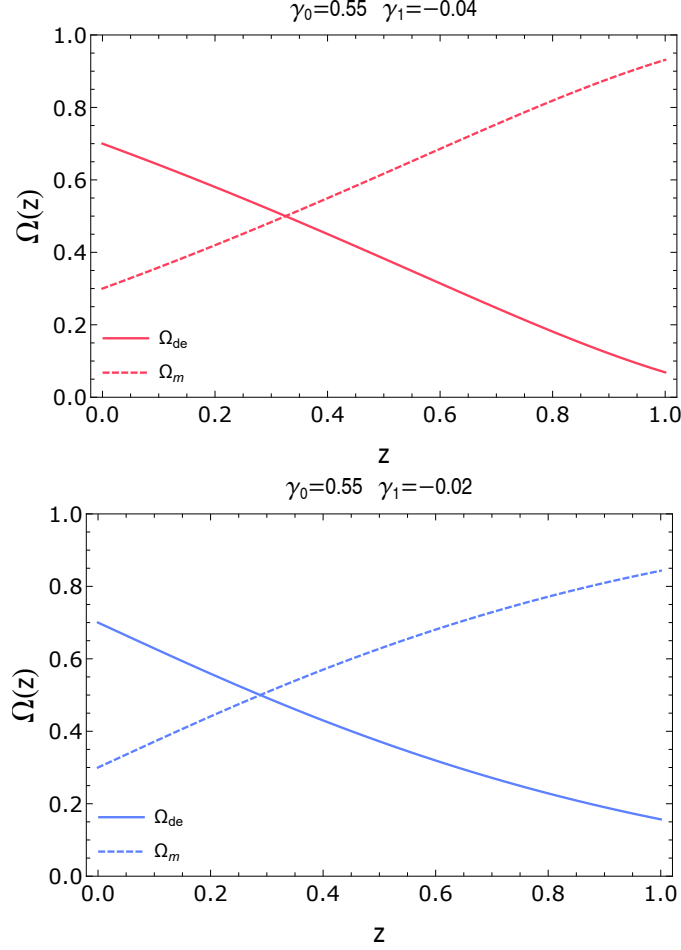


Fig. 3. Normalized densities,  $\Omega_m, \Omega_{DE} = 1 - \Omega_m$ , versus red-shift,  $z$ , setting  $\Omega_{m,0} = 0.3, \gamma_0 = 0.55$ . **TOP:** Normalized densities for  $\gamma_1 = -0.04$ . **BOTTOM:** Normalized densities for  $\gamma_1 = -0.02$ . In both panels solid curves correspond to dark energy, whereas dashed curves correspond to matter.

the curves are displaced upwards as  $\gamma_0$  increases. Furthermore, using the relatively new constraint on  $q_0$ ,  $q_0 = -0.5 \pm 0.08$ , coming from standard sirens, we obtained the allowed range for  $\gamma_1$  for a given set of parameters ( $\gamma_0 = 0.55, \Omega_{m,0} = 0.3$ ). In addition, for viable models we found that DE is either phantom or  $w(z)$  crosses the -1 line from initially very negative values (phantom), ending with a present day value  $w_0 > -1$  (quintessence). This behavior, called quintom in the literature, may be obtained at the level of a Lagrangian description introducing two real scalar fields, one of which enters with the wrong sign in front of the kinetic term. Finally, we showed that an analytic expression for the DE equation-of-state parameter may be obtained in the form of Padé DE parameterizations, and that the order of the

Padé approximation must be at least (4,4).

### Acknowledgements

The author G. P. thanks the Fundação para a Ciência e Tecnologia (FCT), Portugal, for the financial support to the Center for Astrophysics and Gravitation-CENTRA, Instituto Superior Técnico, Universidade de Lisboa, through the Grants No. UID/FIS/00099/2020 and No. PTDC/FIS-AST/28920/2017. L. E. C. acknowledges partial support from the Center of Excellence in Astrophysics and Associated Technologies (PFB06, CONICYT).

### References

1. A. G. Riess et al. *Astron. J.* **116**, 1009 (1998).
2. S. Perlmutter et al., *Astrophys. J.* **517**, 565 (1999).
3. W. L. Freedman and M. S. Turner, *Rev. Mod. Phys.* **75** (2003) 1433 [astro-ph/0308418].
4. A. Einstein, *Annalen Phys.* **49** (1916) 769822.
5. A. Einstein, *Sitzungsber. Preuss. Akad. Wiss. Berlin (Math. Phys. )* **1917** (1917) 142.
6. S. M. Carroll, *Living Rev. Rel.* **4** (2001) 1 [astro-ph/0004075].
7. S. Weinberg, *Rev. Mod. Phys.* **61** (1989) 1.
8. Y. B. Zeldovich, *JETP Lett.* **6** (1967) 316 [*Pisma Zh. Eksp. Teor. Fiz.* **6** (1967) 883].
9. B. Ryden, *Nature Phys.* **13** (2017) no.3, 314.
10. L. Verde, P. Protopapas and R. Jimenez, *Phys. Dark Univ.* **2** (2013) 166 [arXiv:1306.6766 [astro-ph.CO]].
11. K. Bolejko, *Phys. Rev. D* **97** (2018) no.10, 103529.
12. E. Mortsell and S. Dhawan, arXiv:1801.07260 [astro-ph.CO].
13. P. A. R. Ade *et al.* [Planck Collaboration], *Astron. Astrophys.* **594** (2016) A13 [arXiv:1502.01589 [astro-ph.CO]].
14. N. Aghanim *et al.* [Planck Collaboration], arXiv:1807.06209 [astro-ph.CO].
15. A. G. Riess *et al.*, *Astrophys. J.* **826** (2016) no.1, 56 [arXiv:1604.01424 [astro-ph.CO]].
16. A. G. Riess *et al.*, *Astrophys. J.* **861** (2018) no.2, 126 [arXiv:1804.10655 [astro-ph.CO]].
17. E. Mortsell and S. Dhawan, *JCAP* **1809** (2018) no.09, 025 [arXiv:1801.07260 [astro-ph.CO]].
18. V. Poulin, T. L. Smith, T. Karwal and M. Kamionkowski, *Phys. Rev. Lett.* **122** (2019) no.22, 221301 [arXiv:1811.04083 [astro-ph.CO]].
19. P. D. Alvarez, B. Koch, C. Laporte and Á. Rincón, *JCAP* **06** (2021), 019 [arXiv:2009.02311 [gr-qc]].
20. L. Perivolaropoulos and F. Skara, [arXiv:2105.05208 [astro-ph.CO]].
21. Schutz, B. F. 1986, *Nature*, 323, 310.
22. S. Nissanke, D. E. Holz, N. Dalal, S. A. Hughes, J. L. Sievers and C. M. Hirata, [arXiv:1307.2638 [astro-ph.CO]].
23. S. M. Feeney, H. V. Peiris, A. R. Williamson, S. M. Nissanke, D. J. Mortlock, J. Alsing and D. Scolnic, *Phys. Rev. Lett.* **122** (2019) no.6, 061105 [arXiv:1802.03404 [astro-ph.CO]].
24. B. P. Abbott *et al.* [LIGO Scientific, Virgo, 1M2H, Dark Energy Camera GW-E, DES, DLT40, Las Cumbres Observatory, VINROUGE and MASTER], *Nature* **551** (2017) no.7678, 85-88 [arXiv:1710.05835 [astro-ph.CO]].
25. T. P. Sotiriou and V. Faraoni, *Rev. Mod. Phys.* **82** (2010) 451 [arXiv:0805.1726 [gr-qc]].

26. A. De Felice and S. Tsujikawa, *Living Rev. Rel.* **13** (2010) 3 [arXiv:1002.4928 [gr-qc]].
27. W. Hu and I. Sawicki, *Phys. Rev. D* **76** (2007) 064004 [arXiv:0705.1158 [astro-ph]].
28. A. A. Starobinsky, *JETP Lett.* **86** (2007) 157
29. D. Langlois, *Prog. Theor. Phys. Suppl.* **148** (2003) 181 [hep-th/0209261].
30. R. Maartens, *Living Rev. Rel.* **7** (2004) 7 [gr-qc/0312059].
31. G. R. Dvali, G. Gabadadze and M. Porrati, *Phys. Lett. B* **485** (2000) 208 [hep-th/0005016].
32. C. Brans and R. H. Dicke, *Phys. Rev.* **124** (1961) 925.
33. C. H. Brans, *Phys. Rev.* **125**, 2194 (1962).
34. J. C. B. Sanchez and L. Perivolaropoulos, *Phys. Rev. D* **81** (2010) 103505 [arXiv:1002.2042 [astro-ph.CO]].
35. G. Panotopoulos and Á. Rincón, *Eur. Phys. J. C* **78** (2018) no.1, 40 [arXiv:1710.02485 [astro-ph.CO]].
36. B. Ratra and P. J. E. Peebles, *Phys. Rev. D* **37** (1988) 3406.
37. G. Alestas, L. Kazantzidis and L. Perivolaropoulos, *Phys. Rev. D* **101** (2020) no.12, 123516 [arXiv:2004.08363 [astro-ph.CO]].
38. A. Bouali, I. Albarran, M. Bouhmadi-López and T. Ouali, *Phys. Dark Univ.* **26** (2019), 100391 [arXiv:1905.07304 [astro-ph.CO]].
39. A. R. Amani, *Int. J. Theor. Phys.* **50** (2011), 3078-3088.
40. G. Leon, A. Paliathanasis and J. L. Morales-Martínez, *Eur. Phys. J. C* **78** (2018) no.9, 753 [arXiv:1808.05634 [gr-qc]].
41. J. S. Bagla, H. K. Jassal and T. Padmanabhan, *Phys. Rev. D* **67** (2003) 063504 [astro-ph/0212198].
42. C. Armendariz-Picon, V. F. Mukhanov and P. J. Steinhardt, *Phys. Rev. D* **63** (2001) 103510 [astro-ph/0006373].
43. E. J. Copeland, M. Sami and S. Tsujikawa, *Int. J. Mod. Phys. D* **15** (2006) 1753 [hep-th/0603057].
44. A. A. Starobinsky, *JETP Lett.* **68**, 757 (1998).
45. D. Polarski and R. Gannouji, *Phys. Lett. B* **660** (2008), 439-443 [arXiv:0710.1510 [astro-ph]].
46. D. Huterer and E. V. Linder, *Phys. Rev. D* **75** (2007), 023519 [arXiv:astro-ph/0608681 [astro-ph]].
47. C. Di Porto and L. Amendola, *Phys. Rev. D* **77** (2008), 083508 [arXiv:0707.2686 [astro-ph]].
48. A. Kiakotou, O. Elgaroy and O. Lahav, *Phys. Rev. D* **77** (2008), 063005 [arXiv:0709.0253 [astro-ph]].
49. S. Nesseris and L. Perivolaropoulos, *Phys. Rev. D* **77** (2008), 023504 [arXiv:0710.1092 [astro-ph]].
50. L. Wang, P. J. Steinhardt, *Astrophys. J.* **508**, 483 (1998).
51. A. F. Heavens, T. D. Kitching and L. Verde, *Mon. Not. Roy. Astron. Soc.* **380** (2007), 1029-1035 [arXiv:astro-ph/0703191 [astro-ph]].
52. D. Huterer and D. L. Shafer, *Rept. Prog. Phys.* **81** (2018) no.1, 016901 [arXiv:1709.01091 [astro-ph.CO]].
53. V. Mukhanov, *Physical Foundations of Cosmology*, Cambridge University Press (Cambridge, England).
54. R. de Putter, D. Huterer and E. V. Linder, *Phys. Rev. D* **81** (2010) 103513 [arXiv:1002.1311 [astro-ph.CO]].
55. I. Albarran, M. Bouhmadi-Lpez and J. Morais, *Phys. Dark Univ.* **16** (2017) 94 [arXiv:1611.00392 [astro-ph.CO]].
56. G. Panotopoulos, *Phys. Rev. D* **96** (2017) no.2, 023520 [arXiv:1706.10211 [astro-

- ph.CO]].
57. G. Panotopoulos and A. Rincon, Phys. Rev. D **97** (2018) no.10, 103509 [arXiv:1804.11208 [astro-ph.CO]].
  58. L. R. Abramo, R. C. Batista, L. Liberato and R. Rosenfeld, JCAP **0711** (2007) 012 [arXiv:0707.2882 [astro-ph]].
  59. S. Nesseris and L. Perivolaropoulos, Phys. Rev. D **77** (2008) 023504 [arXiv:0710.1092 [astro-ph]].
  60. M. Ishak, Living Rev. Rel. **22** (2019) no.1, 1 [arXiv:1806.10122 [astro-ph.CO]].
  61. M. R. Setare and E. N. Saridakis, Phys. Rev. D **79** (2009), 043005 [arXiv:0810.4775 [astro-ph]].
  62. E. N. Saridakis, Nucl. Phys. B **830** (2010), 374-389 [arXiv:0903.3840 [astro-ph.CO]].
  63. Pade, H. 1892, Ann. Sci. Ecole Norm. Sup., 9(3), 1.
  64. M. Rezaei, Mon. Not. Roy. Astron. Soc. **485** (2019) no.4, 4841-4851 [arXiv:1904.02785 [gr-qc]].
  65. M. K. Mak, C. S. Leung and T. Harko, Mod. Phys. Lett. A **36** (2021) no.06, 2150038 [arXiv:2012.08239 [gr-qc]].
  66. M. Rezaei, M. Malekjani, S. Basilakos, A. Mehrabi and D. F. Mota, Astrophys. J. **843** (2017) no.1, 65 [arXiv:1706.02537 [astro-ph.CO]].
  67. A. Mehrabi and S. Basilakos, Eur. Phys. J. C **78** (2018) no.11, 889 doi:10.1140/epjc/s10052-018-6368-x [arXiv:1804.10794 [astro-ph.CO]].
  68. F. Piazza, H. Steigerwald and C. Marinoni, JCAP **05** (2014), 043 [arXiv:1312.6111 [astro-ph.CO]].